

# Soft Modes, Resonances and Quantum Transport<sup>\*</sup>

Yu. B. Ivanov<sup>†</sup>, J. Knoll, H. van Hees, D. N. Voskresensky<sup>‡</sup>

June 2, 2000

*Gesellschaft für Schwerionenforschung mbH, Planckstr. 1, 64291 Darmstadt, Germany*

## Abstract

Effects of the propagation of particles, which have a finite life-time and an according width in their mass spectrum, are discussed in the context of transport description. First, the importance of coherence effects (Landau–Pomeranchuk–Migdal effect) on production and absorption of field quanta in non-equilibrium dense matter is considered. It is shown that classical diffusion and Langevin results correspond to re-summation of certain field-theory diagrams formulated in terms of full non-equilibrium Green’s functions. Then the general properties of broad resonances in dense and hot systems are discussed in the framework of a self-consistent and conserving  $\Phi$ -derivable method of Baym at the examples of the  $\rho$ -meson in hadronic matter and the pion in dilute nuclear matter. Further we address the problem of a transport description that properly accounts for the damping width of the particles. The  $\Phi$ -derivable method generalized to the real-time contour provides a self-consistent and conserving kinetic scheme. We derive a generalized expression for the non-equilibrium kinetic entropy flow, which includes corrections from fluctuations and mass-width effects. In special cases an  $H$ -theorem is proved. Memory effects in collision terms give contributions to the kinetic entropy flow that in the Fermi-liquid case recover the famous bosonic type  $T^3 \ln T$  correction to the specific heat of liquid Helium-3. At the example of the pion-condensate phase transition in dense nuclear matter we demonstrate important part played by the width effects within the quantum transport.

Quasiparticle representations in many-body theory were designed by Landau, Migdal, Galitsky and others, see refs [1, 2, 3, 4]. This concept was first elaborated at the example of low-lying particle-hole excitations in Fermi liquids. A.B. Migdal was the first to apply these methods to description of various nuclear phenomena and construction of a closed semi-microscopic approach that is now usually called ”Theory of finite Fermi systems” [3].

---

<sup>\*</sup>submitted to Phys. At. Nucl. (Rus.), the volume dedicated to the memory of A.B. Migdal

<sup>†</sup>permanent address: *Kurchatov Institute, Kurchatov sq. 1, Moscow 123182, Russia*

<sup>‡</sup>permanent address: *Moscow Institute for Physics and Engineering, Kashirskoe sh. 31, Moscow 115409, Russia*

The need for explicit treatment of soft modes within this approach stimulated him to generalize this concept to include pion and  $\Delta$  excitations. A.B. Migdal suggested variety of interesting effects like softening of the pion mode in nuclei, pion condensation in dense nuclear and neutron star matter and possible existence of abnormal nuclei glued by pion condensate [5, 6, 7, 8]. These ideas stimulated further development of pion physics with applications to many phenomena in atomic nuclei, neutron stars and heavy-ion collisions, see [8, 9, 10] and refs therein. In this paper we would like to briefly review recent developments of some of the above ideas as applied to heavy-ion physics.

With the aim to describe the collision of two nuclei at intermediate and high energies one is confronted with the fact that the dynamics has to include particles like the in-medium excitation with the pion quantum numbers, as well as the delta and rho-meson resonances with life-times of less than 2 fm/c or equivalently with damping widths above 100 MeV. Also the collisional damping rates deduced from presently used transport codes are of the same order, whereas typical mean temperatures range between 50 to 150 MeV depending on beam energy. Thus, the damping width of most of the constituents in the system can by no means be treated as a perturbation. As a consequence the mass spectrum of the particles in the dense matter is no longer a sharp delta function but rather acquires a width due to collisions and decays. One thus comes to a picture which unifies *resonances*, which have already a width in vacuum due to decay modes, with the "states" of particles in dense matter, which obtain a width due to collisions (collisional broadening). Landau, Pomeranchuk and Migdal were first to demonstrate importance of finite-width effects in multi-particle scattering [11, 12]. Such a coherence scattering effect, known now as Landau–Pomeranchuk–Migdal effect, was recently observed at Stanford accelerator [13].

The theoretical concepts for a proper many-body description in terms of a real time non-equilibrium field theory have been devised by Schwinger [14], Kadanoff and Baym [15], and Keldysh [16] in the early sixties. However a proper dynamical scheme in terms of a transport concept that deals with unstable particles, like resonances, is still lacking. Rather ad-hoc recipes are in use that sometimes violate basic requirements as given by fundamental symmetries and conservation laws, detailed balance or thermodynamic consistency. The problem of conserving approximation has first been addressed by Baym and Kadanoff [17, 18]. They started from an equilibrium description in the imaginary-time formalism and discussed the response to external disturbances. Baym, in particular, showed [18] that any approximation, in order to be conserving, must be so-called  $\Phi$ -derivable. It turned out that the  $\Phi$  functional required is precisely the auxiliary functional introduced by Luttinger and Ward [19] (see also ref. [20]) in connection with the thermodynamic potential. In non-equilibrium case the problem of conserving approximations is even more severe than in near-equilibrium linear-response theory [21, 22].

In this review we discuss recent developments of the transport theory beyond the quasiparticle approximation and consequences of the propagation of particles with short life-times in hadron matter. First we consider few examples of equilibrium systems which clearly indicate that treatment beyond the quasiparticle approximation is really needed. We start with a genuine problem related to the occurrence of broad damping width, i.e. the soft-mode problem (Landau–Pomeranchuk–Migdal effect). This is the direct radiation

of quanta from a piece of a dense medium [23]. Classically this problem is formulated as coupling of a coherent classical field, e.g., the Maxwell field, to a stochastic source described by the Brownian motion of a charged particle. In this case the classical current-current correlation function, can be obtained in closed analytical terms and discussed as a function of the macroscopic transport properties, the friction and diffusion coefficient of the Brownian particle. We show that this result corresponds to a partial re-summation of photon self-energy diagrams in the real-time formulation of field theory. Subsequently, properties of particles with broad damping width are illustrated at the examples of the  $\rho$ -meson in dense matter at finite temperature [24] and the pion in the limit of a dilute nuclear matter [25]. The question of consistency becomes especially important for a multi-component system like  $\pi N \Delta \rho, \dots$ , where the properties of one species can change due to the presence of interactions with the others and *vice versa*. The "*vice versa*" is very important and corresponds to the principle of *actio = re-actio*. This implies that the self-energy of one species cannot be changed through the interaction with other species without affecting the self-energies of the latter ones also. The  $\Phi$ -derivable method of Baym [18] offers a natural and consistent way to account for this principle.

Then we address the question how particles with broad mass-width can be described consistently within a transport picture [21, 22]. We argue that the Kadanoff–Baym equations in the first gradient approximation together with the  $\Phi$ -functional method of Baym [18] provide a proper self-consistent approach for kinetic description of systems of particles with a broad mass-width. We argue that after gradient expansion the full set of equations describing quantum transport contains two equations, the differential generalized kinetic equation for a distribution function in  $8-(X, p)$ -space and the algebraic equation for the spectral density. Other equations are resolved. We discuss the problems of concerning charge and energy–momentum conservation, thermodynamic consistency, memory effects in the collision term and the growth of entropy in specific cases. Finally, we demonstrate finite-width effects in quantum kinetic description at the example of pion condensation, where the width of soft pionic excitations due to their decay into particle-hole pairs governs the dynamics of the phase transition in the isospin-symmetric nuclear matter.

We use the units  $\hbar = c = 1$ . For simplicity we treat fermions non-relativistically whereas bosons (mesons) are treated as relativistic particles.

## 1 Bremsstrahlung from Classical Sources

For a clarification of the soft mode problem following [23] we first discuss an example in classical electrodynamics. We consider a stochastic source, the hard matter, where the motion of a single charge is described by a diffusion process in terms of a Fokker–Planck equation for the probability distribution  $f$  of position  $\mathbf{x}$  and velocity  $\mathbf{v}$

$$\frac{\partial}{\partial t} f(\mathbf{x}, \mathbf{v}, t) = \left( D \Gamma_x^2 \frac{\partial^2}{\partial \mathbf{v}^2} + \Gamma_x \frac{\partial}{\partial \mathbf{v}} \mathbf{v} - \mathbf{v} \frac{\partial}{\partial \mathbf{x}} \right) f(\mathbf{x}, \mathbf{v}, t). \quad (1)$$

Fluctuations also evolve in time according to this equation, or equivalently by a random walk process [23], and this way determine correlations. This charge is coupled to the

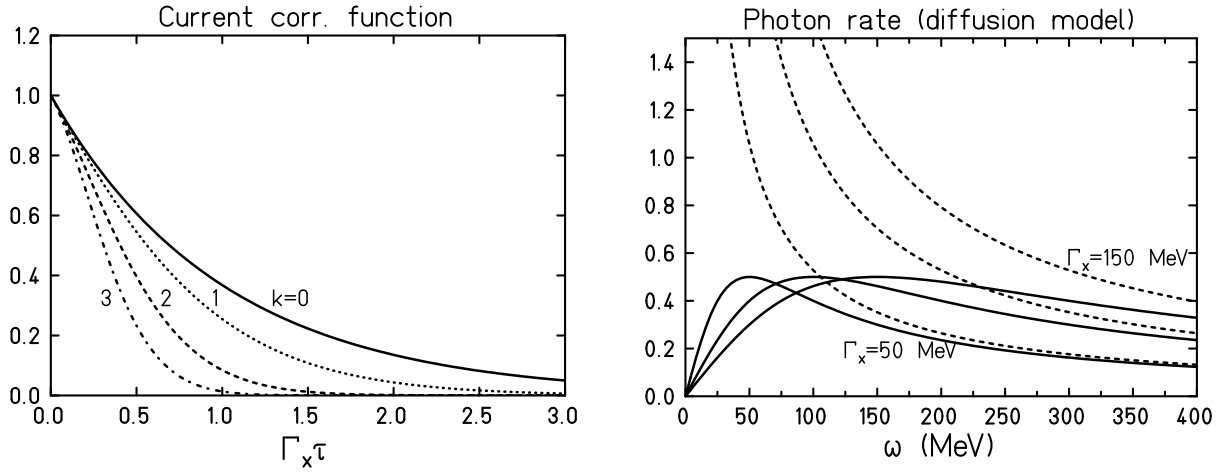


Figure 1: Left: Current-current correlation function in units of  $e^2 \langle v^2 \rangle$  as a function of time (in units of  $1/\Gamma_x$ ) for different values of the photon momentum  $q^2 = 3k^2\Gamma_x^2/\langle v^2 \rangle$  with  $k = 0, 1, 2, 3$ . Right: Rate of real photons  $d^2N/(d\omega dt)$  in units of  $4\pi e^2 \langle v^2 \rangle / 3$  for a non-relativistic source for  $\Gamma_x = 50, 100, 150$  MeV; for comparison the IQF results (dashed lines) are also shown.

Maxwell field. On the assumption of a non-relativistic source, this case does not suffer from standard pathologies encountered in hard thermal loop (HTL) problems of QCD, namely the collinear singularities, where  $\mathbf{v}\mathbf{q} \approx 1$ , and from diverging Bose-factors. The advantage of this Abelian example is that damping can be fully included without violating current conservation and gauge invariance. This problem is related to the Landau-Pomeranchuk-Migdal effect of bremsstrahlung in high-energy scattering [11, 12].

The two macroscopic parameters, the spatial diffusion  $D$  and friction  $\Gamma_x$  coefficients determine the relaxation rates of velocities. In the equilibrium limit ( $t \rightarrow \infty$ ) the distribution attains a Maxwell-Boltzmann velocity distribution with the temperature  $T = m \langle v^2 \rangle / 3 = mD\Gamma_x$ . The correlation function can be obtained in closed form and one can discuss the resulting time correlations of the current at various values of the spatial photon momentum  $\mathbf{q}$ , Fig. 1 (details are given in ref. [23]). For the transverse part of the correlation tensor this correlation decays exponentially as  $\sim e^{-\Gamma_x \tau}$  at  $\mathbf{q} = 0$ , and its width further decreases with increasing momentum  $q = |\mathbf{q}|$ . The in-medium production rate is given by the time Fourier transform  $\tau \rightarrow \omega$ , Fig. 1 (right part). The hard part of the spectrum behaves as intuitively expected, namely, it is proportional to the microscopic collision rate expressed through  $\Gamma_x$  (cf. below) and thus can be treated perturbatively by incoherent quasi-free (IQF) scattering prescriptions. However, independently of  $\Gamma_x$  the rate saturates at a value of  $\sim 1/2$  in these units around  $\omega \sim \Gamma_x$ , and the soft part shows the inverse behavior. That is, with increasing collision rate the production rate is more and more suppressed! This is in line with the picture, where photons cannot resolve the individual collisions any more. Since the soft part of the spectrum behaves like  $\omega/\Gamma_x$ , it shows a genuine non-perturbative feature which cannot be obtained by any power series in  $\Gamma_x$ . For comparison: the dashed lines show the corresponding IQF yields, which agree with the correct rates for the hard part while completely fail and diverge towards the soft

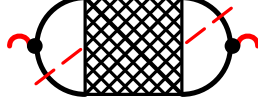


Figure 2: Self-energy diagrams determining the production and absorption rates.

end of the spectrum. For non-relativistic sources  $\langle v^2 \rangle \ll 1$  one can ignore the additional  $q$ -dependence (dipole approximation; cf. Fig. 1) and the entire spectrum is determined by one macroscopic scale, the relaxation rate  $\Gamma_x$ . This scale provides a quenching factor

$$C_0(\omega) = \frac{\omega^2}{\omega^2 + \Gamma_x^2} \quad (2)$$

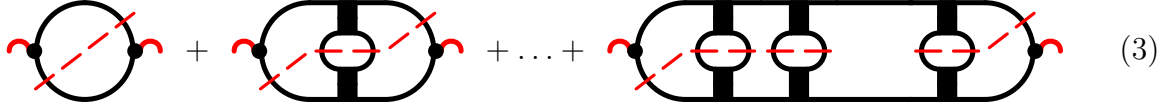
by which the IQF results have to be corrected in order to account for the finite collision time effects in dense matter.

The diffusion result represents a re-summation of the microscopic Langevin multiple collision picture and altogether only macroscopic scales are relevant for the form of the spectrum and not the details of the microscopic collisions. Note also that the classical result fulfills the classical version ( $\hbar \rightarrow 0$ ) of the sum rules discussed in refs. [26, 23].

## 2 Radiation at the Quantum Level

We have seen that at the classical level the problem of radiation from dense matter can be solved quite naturally and completely at least for simple examples, and Figs. 1 display the main physics. They show, that the *damping* of the particles due to scattering is an important feature, which in particular has to be included right from the onset. This does not only assure results that no longer diverge, but also provides a systematic and convergent scheme. On the *quantum level* such problems require techniques beyond the standard repertoire of perturbation theory or the quasi-particle approximation. In terms of non-equilibrium diagrammatic technique in Keldysh notation, the production or absorption rates are given by the self-energy diagrams of the type presented in Fig. 2 with an in- and out-going radiating particle (e.g. photon) line [27, 23]. The hatched loop area denotes all strong interactions of the source. The latter give rise to a whole series of diagrams. As mentioned, for the particles of the source, e.g. the nucleons, one has to re-sum Dyson's equation with the corresponding full complex self-energy in order to determine the full Green's functions in dense matter. Once one has these Green's functions together with the interaction vertices at hand, one could in principle calculate the required diagrams. However, both the computational effort to calculate a single diagram and the number of diagrams increase dramatically with the loop order of the diagrams, such that in practice only lowest-order loop diagrams can be considered in the quantum case. In certain limits some diagrams drop out. We could show that in the *classical limit*, which in this case implies the hierarchy  $\omega, |\mathbf{q}|, \Gamma \ll T \ll m$  together with low phase-space occupations for the source, i.e.  $f(x, p) \ll 1$ , only the following set of

diagrams survives



$$(3)$$

In these diagrams the bold lines denote the full nucleon Green's functions which also include the damping width, the black blocks represent the effective nucleon-nucleon interaction in matter, and the full dots, the coupling vertex to the photon. The thin dashed lines show how the diagrams are to be cut into two interfering amplitudes. This way each of these diagrams with  $n$  interaction loop insertions just corresponds to the  $n^{th}$  term in the corresponding classical Langevin process, where hard scatterings occur at random with a constant *mean collision rate*  $\Gamma$ . These scatterings consecutively change the velocity of a point charge from  $\mathbf{v}_0$  to  $\mathbf{v}_1$ , to  $\mathbf{v}_2$ ,  $\dots$ . In between scatterings the charge moves freely. For such a multiple collision process the space integrated current-current correlation function takes a simple Poisson form

$$\begin{aligned} i\Pi^{\mu\nu-+} &\propto \int d^3x_1 d^3x_2 \langle j^\nu(\mathbf{x}_1, t - \frac{\tau}{2}) j^\mu(\mathbf{x}_2, t + \frac{\tau}{2}) \rangle \\ &= e^2 \langle v^\mu(0) v^\nu(\tau) \rangle = e^2 e^{-|\Gamma\tau|} \sum_{n=0}^{\infty} \frac{|\Gamma\tau|^n}{n!} \langle v_0^\mu v_n^\nu \rangle \end{aligned} \quad (4)$$

with  $v = (1, \mathbf{v})$ . Here  $\langle \dots \rangle$  denotes the average over the discrete collision sequence. This form, which one writes down intuitively, agrees with the analytic result of the quantum correlation diagrams (3) in the limit  $f(x, p) \ll 1$  and  $\Gamma \ll T$ . Fourier transformed it determines the spectrum in completely regular terms (void of any infra-red singularities), where each term describes the interference of the photon being emitted at a certain time or  $n$  collisions later. In special cases where velocity fluctuations are degraded by a constant fraction  $\alpha$  in each collision, such that  $\langle \mathbf{v}_0 \cdot \mathbf{v}_n \rangle = \alpha^n \langle \mathbf{v}_0 \cdot \mathbf{v}_0 \rangle$ , one can re-sum the whole series in Eq. (4) and thus recover the relaxation result with  $2\Gamma_x \langle \mathbf{v}^2 \rangle = \Gamma \langle (\mathbf{v}_0 - \mathbf{v}_1)^2 \rangle$  at least for  $\mathbf{q} = 0$  and the corresponding quenching factor (2). Thus the classical multiple collision example provides a quite intuitive picture about such diagrams. Further details can be found in ref. [23].

The above example shows that we have to deal with particle transport that explicitly takes account of the particle mass-width in order to properly describe soft radiation from the system.

### 3 The $\rho$ -meson in Dense Matter

Following  $\Phi$  derivable scheme we will first discuss two examples within thermo-equilibrium systems. First we will concern properties of the  $\rho$ -meson and their consequences for the  $\rho$ -decay into di-leptons [24]. In terms of the non-equilibrium diagrammatic technique, the

exact production rate of di-leptons is given by the following formula

$$\frac{dn^{e^+e^-}}{dtdm} = \text{[Feynman diagram: two incoming lines from the left and two outgoing lines to the right, connected by a horizontal wavy line with a loop in the middle]} = f_\rho(m, \mathbf{p}, \mathbf{x}, t) A_\rho(m, \mathbf{p}, \mathbf{x}, t) 2m \Gamma^{\rho \rightarrow e^+e^-}(m). \quad (5)$$

Here  $\Gamma^{\rho \rightarrow e^+e^-}(m) \propto 1/m^3$  is the mass-dependent electromagnetic decay rate of the  $\rho$  into the di-lepton pair of invariant mass  $m$ . The phase-space distribution  $f_\rho(m, \mathbf{p}, \mathbf{x}, t)$  and the spectral function  $A_\rho(m, \mathbf{p}, \mathbf{x}, t)$  define the properties of the  $\rho$ -meson at space-time point  $\mathbf{x}, t$ . Both quantities are in principle to be determined dynamically by an appropriate transport model. However till to-date the spectral functions are not treated dynamically in most of the present transport models. Rather one employs on-shell  $\delta$ -functions for all stable particles and spectral functions fixed to the vacuum shape for resonances.

As an illustration, we follow the two channel example presented by one of us in ref. [28]. There the  $\rho$ -meson just strongly couples to two channels, i.e. the  $\pi^+\pi^-$  and  $\pi N \leftrightarrow \rho N$  channels, the latter being relevant at finite nuclear densities. The latter component is representative for all channels contributing to the so-called *direct*  $\rho$  in transport codes. For a first orientation the equilibrium properties<sup>1</sup> are discussed in simple analytical terms with the aim to discuss the consequences for the implementation of such resonance processes into dynamical transport simulation codes.

Both considered processes add to the total width of the  $\rho$ -meson

$$\Gamma_{\text{tot}}(m, \mathbf{p}) = \Gamma_{\rho \rightarrow \pi^+\pi^-}(m, \mathbf{p}) + \Gamma_{\rho \rightarrow \pi N N^{-1}}(m, \mathbf{p}), \quad (6)$$

and the equilibrium spectral function then results from the cuts of the two diagrams

$$A_\rho(m, \mathbf{p}) = \text{[Feynman diagram: wavy line, dashed loop, wavy line]} + \text{[Feynman diagram: wavy line, solid loop, wavy line]} \quad (7)$$

$$\underbrace{\hspace{10em}}_{\frac{2m\Gamma_{\rho \rightarrow \pi^+\pi^-} + 2m\Gamma_{\rho \rightarrow \pi N N^{-1}}}{(m^2 - m_\rho^2 - \text{Re}\Sigma^R)^2 + m^2\Gamma_{\text{tot}}^2}}$$

In principle, both diagrams have to be calculated in terms of fully self-consistent propagators, i.e. with corresponding widths for all particles involved. This formidable task has not been done yet. Using micro-reversibility and the properties of thermal distributions,

---

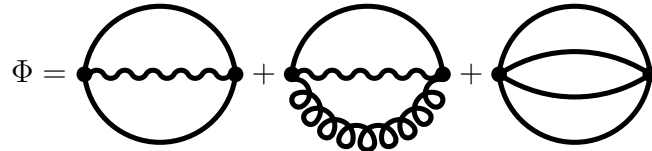
<sup>1</sup>Far more sophisticated calculations have already been presented in the literature [29, 30, 31, 32, 33, 34]. It is not the point to compete with them at this place.

the two terms in Eq. (7) contributing to the di-lepton yield (5), can indeed approximately be reformulated as the thermal average of a  $\pi^+\pi^- \rightarrow \rho \rightarrow e^+e^-$ -annihilation process and a  $\pi N \rightarrow \rho N \rightarrow e^+e^- N$ -scattering process, i.e.

$$\frac{dn^{e^+e^-}}{dm dt} \propto \left\langle f_{\pi^+} f_{\pi^-} v_{\pi\pi} \sigma(\pi^+\pi^- \rightarrow \rho \rightarrow e^+e^-) + f_{\pi} f_N v_{\pi N} \sigma(\pi N \rightarrow \rho N \rightarrow e^+e^- N) \right\rangle_T, \quad (8)$$

where  $f_{\pi}$  and  $f_N$  are corresponding particle occupations and  $v_{\pi\pi}$  and  $v_{\pi N}$  are relative velocities. However, the important fact to be noticed is that in order to preserve unitarity the corresponding cross sections are no longer the free ones, as given by the vacuum decay width in the denominator, but rather involve the *medium dependent total width* (6). This illustrates in simple terms that rates of broad resonances can no longer simply be added in a perturbative way. Since it concerns a coupled channel problem, there is a cross talk between the different channels to the extent that the common resonance propagator attains the total width arising from all partial widths feeding and depopulating the resonance. While a perturbative treatment with free cross sections in Eq. (8) would enhance the yield at resonance mass,  $m = m_{\rho}$ , if a channel is added, cf. Fig. 3 left part, the correct treatment (7) even inverts the trend and indeed depletes the yield at resonance mass, right part in Fig. 3. Furthermore, one sees that only the total yield involves the spectral function, while any partial cross section refers to that partial term with the corresponding partial width in the numerator! Unfortunately so far all these facts have been ignored or even overlooked in the present transport treatment of broad resonances. Compared to the spectral function both thermal components in Fig. 3 show a significant enhancement on the low mass side and a strong depletion at high masses due to the thermal weight  $f \propto \exp(-p_0/T)$  in the rate (5).

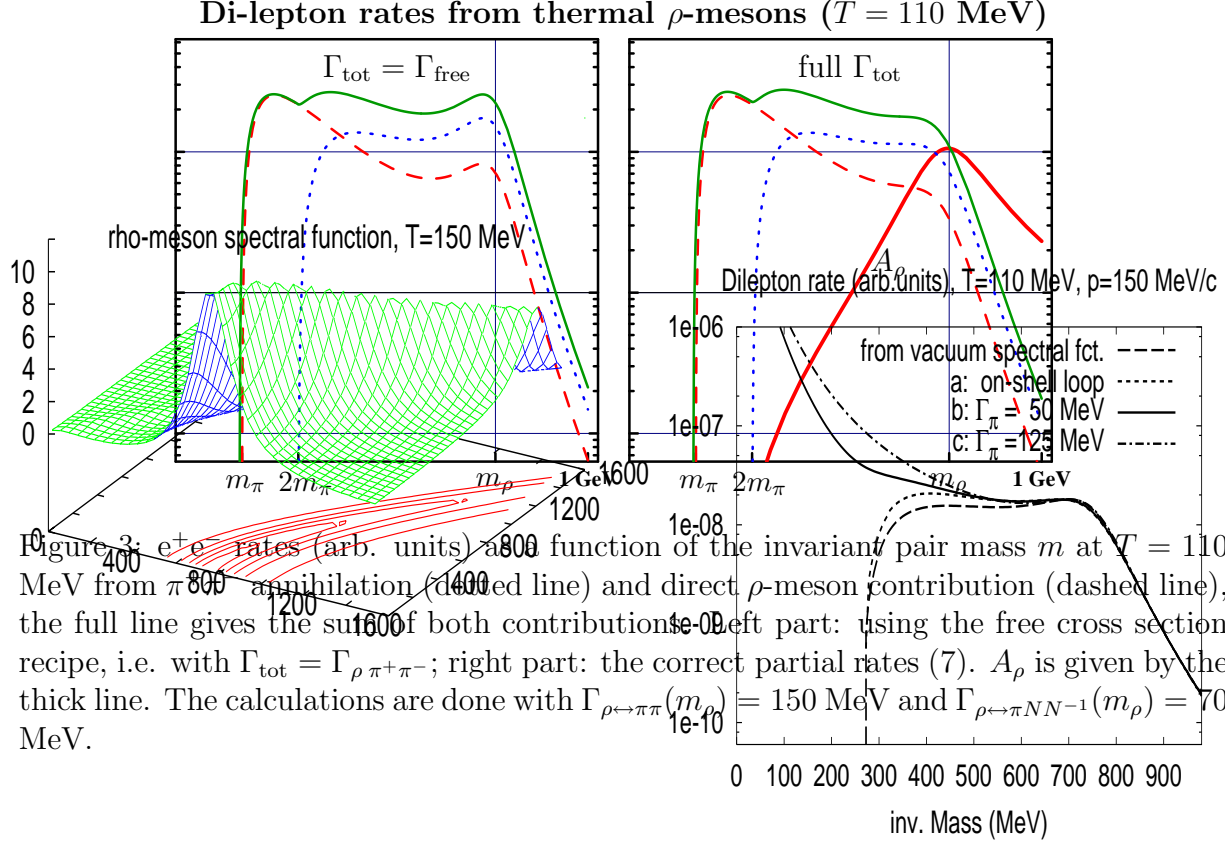
As an example we show an exploratory study of the interacting system of  $\pi$ ,  $\rho$  and  $a_1$ -mesons described by the  $\Phi$ -functional



$$\Phi = \text{[Diagram 1]} + \text{[Diagram 2]} + \text{[Diagram 3]} \quad (9)$$

(cf. section 5 below). The couplings and masses are chosen as to reproduce the known vacuum properties of the  $\rho$  and  $a_1$  meson with nominal masses and widths  $m_{\rho} = 770$  MeV,  $m_{a_1} = 1200$  MeV,  $\Gamma_{\rho} = 150$  MeV,  $\Gamma_{a_1} = 400$  MeV. The results of a finite temperature calculation at  $T = 150$  MeV with all self-energy loops resulting from the  $\Phi$ -functional of Eq. (9) computed [24] with self-consistent broad width Green's functions are displayed in Fig. 4 (corrections to the real part of the self-energies were not yet included). The last diagram of  $\Phi$  with the four pion self-coupling has been added in order to supply pion with broad mass-width as they would result from the coupling of pions to nucleons and the  $\Delta$  resonance in nuclear matter environment. As compared to first-order one-loop results which drop to zero below the 2-pion threshold at 280 MeV, the self-consistent results essentially add in strength at the low-mass side of the di-lepton spectrum.





$|\mathbf{p}|$

$\omega$

Figure 4: Left part: contour plot of the self-consistent spectral function of the  $\rho$ -meson as a function of energy and spatial momentum; right part: thermal di-lepton rate as a function of invariant mass at  $|\mathbf{p}| = 300$  MeV/c